Journal of Applied Polymer Science

# Nanostructured star-shaped polythiophene with tannic acid core: Synthesis, characterization, and its physicochemical properties

**Bakhshali Massoumi,[1] Mehdi Jaymand[2]**

[1]Department of Chemistry, Payame Noor University, Tehran, P.O. Box: 19395-3697, Islamic Republic of Iran

[2]Research Center for Pharmaceutical Nanotechnology, Tabriz University of Medical Sciences, Tabriz, P.O. Box: 51656-65811, Islamic Republic of Iran

Correspondence to: M. Jaymand (E-mail: m.jaymand@yahoo.com or m.jaymand@gmail.com or jaymandm@tbzmed.ac.ir)

**ABSTRACT:** For the first time, synthesis and characterization of a nanostructured star-shaped polythiophene (PTh) with tannic acid core by both chemical and electrochemical oxidation polymerization methods through a "core-first" method is reported. The chemical structures of all samples as representatives were characterized by means of Fourier transform infrared (FTIR), and $^1$H nuclear magnetic resonance (NMR) spectroscopies. The electroactivity behaviors of the synthesized samples were verified under cyclic voltammetric conditions, and their conductivities were determined using the four-probe technique. The synthesized star-shaped PTh showed higher electrical conductivity and electroactivity than those of the PTh in both chemical and electrochemical polymerized samples, due to its large surface area, spherical, and three-dimensional structure. Moreover, the thermal behaviors, optical properties, and morphologies of the synthesized samples were investigated by means of thermogravimetric analysis (TGA), ultraviolet–visible (UV–Vis) spectroscopy, and field emission scanning electron microscopy (FE-SEM), respectively. © 2016 Wiley Periodicals, Inc. J. Appl. Polym. Sci. **2016**, *133*, 43513.

**KEYWORDS:** conducting polymers; electrochemistry; nanostructured polymers; properties and characterization

Received 7 November 2015; accepted 4 February 2016

**DOI: 10.1002/app.43513**

## INTRODUCTION

It is well accepted that, since the discovery of intrinsically conductive polymers (ICPs) in 1977, more and more research efforts have been devoted to the promotion, modification, and application of these polymers, in part due to their unique physicochemical properties.[1–7] Among the large family of these polymers, polyaniline (PANI), polypyrrole (PPy), and polythiophene (PTh) are important members, and could be incorporated in various practical and technological applications due to their stabilities, and exclusive physicochemical properties.[8–11] In addition, these conducting polymers have generated a great deal of interest due to their low-cost synthesis (via electrochemical or chemical oxidation polymerization methods), chemical and electronic properties, unique redox tunability, environmental and thermal stability, and wide range of commercial and technological applications.[1,2,12,13]

It should be pointed out that the polythiophene and its derivatives have attracted remarkable attention in scientific and industrial committees, in part due to combination of their chemical and physical properties. Extensive research efforts have been focused for the exploitations from polythiophenes in various applications such as (bio)chemical sensors,[14] organic photovoltaics (OPVs),[15] organic field-effect transistors (OFETs),[16] rechargeable batteries,[17] organic light emitting diodes (OLEDs),[18] electrical memory performance,[19] biomedical fields,[20] and many more.

As a decisive fact, the bulk properties of the conductive polymers such as electronic, mechanical, chemical, and optical properties can be controlled through the organization of the polymeric chains in the nanometer scale and three-dimension structure. Thus, the controlled synthesis of conducting polymers is of vital importance in modern material science, which has been the subject of many investigations.[21–23] In this respect, star-shaped and dendritic conductive polymers have received significant attention over the past decade due to their unique three-dimensional shape and physicochemical properties. The star-shaped polymers, which are composed of multiple polymer chains emanating from junction points, have stimulated great interest over the past decade due to their ability to pack in three-dimensions. They have possible processing some advantages due to their compact structure in comparison with typical two-dimensional linear analogues.[24,25] For example, in star-shaped conductive polymers the conducting chains surprisingly, can provide sufficient intermolecular overlap to give solid materials with electrical conductivities higher than the corresponding linear counterparts.[26–28]

Since the first report of dendritic polythiophene by Advincula group in 2002,[29] it is well established that these types of

π-conjugated polymers exhibited very interesting three-dimensional supramolecular assemblies, photovoltaic applications, and are good candidates as light-harvesting antenna macromolecules. The spherical and three-dimensional structure of the star-shaped polythiophene gives it the conductive characteristics that are better than the linear counterpart. The stereochemistry of the star-shaped polythiophene chains allows sufficient overlap of π-orbitals.[30–32]

In this work, we explore the synthesis and characterization of nanostructured star-shaped polythiophene with tannic acid core by both chemical and electrochemical oxidation polymerization methods. For this purpose, the tannic acid was functionalized with *p*-anthranilic acid in the presence of *p*-toluenesulfonic acid (*p*-TSA) as the dehydrating agent to produce a phenylamine-functionalized tannic acid (PhATA). Afterwards, a thiophene-functionalized tannic acid macromonomer (ThTAM) was synthesized via a condensation reaction between PhATA and thiophene-2-carbaldehyde. The resultant macromonomer was subsequently used in chemical and electrochemical oxidation polymerization methods with thiophene monomer to produce nanostructured star-shaped polythiophenes.

## EXPERIMENTAL

### Materials

Tannic acid was purchased from Sigma-Aldrich (USA), and was used as received. Thiophene monomer from Merck (Darmstadt, Germany) was distilled under reduced pressure before use. Toluene (Merck) was dried by refluxing over sodium, and distilled under argon prior to use. Magnesium sulfate ($MgSO_4$), thiophene-2-carbaldehyde, *p*-toluenesulfonic acid (*p*-TSA), *p*-anthranilic acid, tetraethylammonium tetrafluoroborate (TEAFB), and anhydrous ferric chloride ($FeCl_3$) were purchased from Merck, and were used as received. All other reagents were purchased from Merck and purified according to standard methods.

### Synthesis of Phenylamine-Functionalized Tannic Acid (PhATA)

A three-neck round-bottom flask equipped with a dean-stark trap, gas inlet/outlet, and a magnetic stirrer, was charged with tannic acid (3.00 g, 1.76 mmol), *p*-anthranilic acid (6.25 g, 45 mmol), and anhydrous toluene (60 mL). A catalytic amount of *p*-TSA (0.10 g, 0.55 mmol) as the dehydrating agent was added to the reaction mixture, and the reaction mixture was de-aerated by bubbling highly pure argon for 10 min. At the end of this period, the reaction mixture was heated up to 120 °C ± 3 for about 24 h. The water of reaction was removed as an azeotrope until no more water was formed. It could mean that the reaction had gone to completion. Then, the reaction flask was cooled to room temperature by ice water bath. The crude product was filtered and dried in vacuum at room temperature. The crude product was purified by recrystallization from acetonitrile ($CH_3CN$) for three times.

### Synthesis of Thiophene-Functionalized Tannic Acid Macromonomer (ThTAM)

The ThTAM macromonomer was synthesized via a condensation reaction between PhATA and thiophene-2-carbaldehyde as follows. In a two-neck round-bottom flask equipped with a gas inlet/outlet and a magnetic stirrer, 3.00 g of PhATA and $MgSO_4$ (5.00 g, 42 mmol) were dissolved in 100 mL of anhydrous toluene. The reaction mixture was de-aerated by bubbling highly pure argon for 10 min and then thiophene-2-carbaldehyde (5 mL, 55 mmol) was added to the flask. The reaction mixture was refluxed at room temperature for about 48 h. At the end of this time, the crude product was filtered, washed several times with toluene to remove residue thiophene-2-carbaldehyde and dried in vacuum at room temperature. Afterwards, the crude product was dissolved in tetrahydrofuran (THF) to remove $MgSO_4$. It is important to note that the synthesized ThTAM macromonomer was completely soluble in THF, while $MgSO_4$ is not soluble in THF. The ThTAM macromonomer was obtained after removing of THF with a rotary evaporator.

### Synthesis of Star-Shaped Polythiophene via Chemical Oxidation Polymerization Method

A 250 mL three-necked round-bottom flask equipped with a condenser, dropping funnel, gas inlet/outlet, and a magnetic stirrer, was charged with ThTAM macromonomer (1.00 g), and dried $CHCl_3$ (90 mL). The mixture was refluxed at 60 °C for about 1 h to completely dissolving of ThTAM macromonomer. At the end of this time, the reaction mixture was cooled to room temperature, added thiophene monomer (3 mL, 38.2 mmol), and then the solution was de-aerated by bubbling highly pure argon for 10 min.

In a separate container, 24.80 g (153 mmol) of anhydrous ferric chloride ($FeCl_3$) was dissolved in 30 mL of dried anhydrous acetonitrile ($CH_3CN$). The solution was de-aerated by bubbling highly pure argon for 10 min and was slowly added to the reaction mixture at a rate of 5 mL $min^{-1}$ under an argon atmosphere. The reaction mixture was refluxed for about 24 h at room temperature under an inert atmosphere. The reaction was terminated by pouring the contents of the flask into a large amount of methanol. The product was filtered and washed several times with methanol. The final dark red solid was dried in vacuum at room temperature. In addition, the PTh was synthesized by the same method, in the absence of the ThTAM macromonomer.

### Synthesis of Star-Shaped Polythiophene via Electrochemical Oxidation Polymerization Method

The star-shaped polythiophene was also synthesized via electrochemical oxidation polymerization method. For this purpose, a 2% (w/v) solution of ThTAM macromonomer was dissolved in THF and both sides of working electrode (Pt) were coated with ThTAM by drop-coating. The electrolysis cell was prepared by dissolving tetraethylammonium tetrafluoroborate (0.1 mol $L^{-1}$) in acetonitrile ($CH_3CN$) and introducing 40 μL of thiophene monomer. Constant potential electrolysis was performed at 2.00 V versus reference electrode (Ag/AgCl) for about 1 h at room temperature under argon atmosphere for successful synthesis of star-shaped polythiophene.

### Characterization

Fourier transform infrared (FTIR) spectra of the samples were collected on a Shimadzu 8101M FTIR (Shimadzu, Kyoto, Japan) between the frequency range of 4000 and 400 $cm^{-1}$, with an attenuated total reflection facility. The samples were prepared by grinding the dry powders with potassium bromide (KBr) and compressing the mixture into disks. The spectra were recorded at room temperature. The $^1H$ nuclear magnetic resonance (NMR) spectra of the samples were recorded at 25 °C using an FT-NMR

(400 MHz) Bruker spectrometer (Bruker, Ettlingen, Germany). The sample for NMR spectroscopy was prepared by dissolving about 10 mg of sample in 1 mL of deuterated dimethylsulfoxide (DMSO-$d_6$), and chemical shifts were reported in parts per million (ppm) units with tetramethylsilane (TMS) as internal standard. The thermal properties of the synthesized samples were investigated by thermogravimetric analyzer (TGA-PL STA 1640 equipment (Polymer Laboratories, Shropshire, UK)). The thermogravimetric analysis (TGA) experiments were conducted under nitrogen atmosphere from room temperature to 750 °C with heating rate of 10 °C $min^{-1}$. Ultraviolet–visible (UV–vis) spectroscopy was conducted using a Shimadzu 1650 PC UV–vis spectrophotometer (Shimadzu, Kyoto, Japan) in the wavelength range 700–250 nm. The field emission scanning electron microscope (FE-SEM) type 1430 VP (LEO Electron Microscopy, Cambridge, UK) was applied to determine the morphologies of the synthesized samples. Electrochemical experiments were conducted using Auto-Lab PGSTA T302N. The electrochemical cell contained five openings: three of them were used for the electrodes (working, counter, and reference) and two for argon bubbling in the solutions during all experiments. The conductivity of the synthesized samples was determined using the four-probe technique (Azar Electrode, Urmia, Iran) at room temperature.

## RESULTS AND DISCUSSION

Studies on the physicochemical properties of the conductive polymers have been a matter of intense investigation in last few decades due to their importance in basic scientific research and potential technology applications. However, it is well established that the physicochemical properties of the conductive polymers can be controlled through the synthetic route. Various synthetic routes such as Grignard metathesis (GRIM) polymerization or transition metal catalyzed cross-coupling reactions,[33] electrosynthesis,[34] and chemical oxidation polymerization methods have been employed for the controlled growth of PTh structure. In the case of dendritic or star-shaped conductive polymers, they have many special characteristics such as large surface area, excellent connectivity and electroactivity, more functional sites, and unique physicochemical properties over to liner analogues. The aim of this study is the synthesis of novel star-shaped polythiophene with tannic acid core by both chemical and electrochemical oxidation polymerization methods as depicted in Schemes 1–3.

### Synthesis of PhATA

The FTIR spectra of the tannic acid, *p*-anthranilic acid and PhATA are shown in Figure 1. The FTIR spectrum of the tannic acid shows the characteristic absorption bands due to the stretching vibrations of hydroxyl groups centered at 3378 $cm^{-1}$, the stretching vibrations of carbonyl groups at 1706 $cm^{-1}$, C=C stretching vibrations (1607 and 1447 $cm^{-1}$), $\gamma$(C–H) in the aromatic ring (865 and 752 $cm^{-1}$), and C–O stretching vibrations at 1312 $cm^{-1}$.[35] It is important to note that the aliphatic and aromatic C–H stretching vibrations are overlapped with the very strong band of the hydroxyl groups.

The FTIR spectrum of the *p*-anthranilic acid shows the characteristic absorption bands due to the stretching vibrations of aromatic C–H (3050–2970 $cm^{-1}$), weak aromatic overtone and combination bands in the 2000–1650 $cm^{-1}$ region, C=C stretching vibrations at 1593 $cm^{-1}$, $\gamma$(C–H) in the aromatic ring (841 and 769 $cm^{-1}$), $–NH_2$ stretching vibrations at 3360 and 3223 $cm^{-1}$, hydroxyl stretching vibration at 3458 $cm^{-1}$, N–H out-of-plane at 895 $cm^{-1}$, the stretching vibration of carbonyl group at 1663 $cm^{-1}$, and C–O stretching vibration at 1287 $cm^{-1}$.

In comparison with the FTIR spectrum of the pure tannic acid, the most significant changes in the FTIR spectrum of the PhATA are the appearance of $–NH_2$ stretching vibrations at 3360 and 3223 $cm^{-1}$, and the stretching vibrations of aromatic C–H at 3050–2970 $cm^{-1}$ region. In addition, as seen in this spectrum the intensity of the hydroxyl stretching vibration is decreased significantly (3458 $cm^{-1}$).

### Synthesis of ThTAM Macromonomer

The FTIR spectrum of the ThTAM macromonomer is shown in Figure 2. The most distinctive feature of the ThTAM macromonomer in comparison with PhATA, in the FTIR spectra are the appearance of strong band at 1576 $cm^{-1}$ (corresponded to C=N groups), and disappearance of stretching vibrations related to the amine groups after reaction of PhATA with thiophene-2-carbaldehyde.

The synthesized ThTAM macromonomer was further characterized by means of $^1$H NMR spectroscopy. The $^1$H NMR spectra of the TA, PhATA, and ThTAM are shown in Figure 3. The aliphatic protons of glucose core of the tannic acid are appeared at 3.00–4.00 ppm. It is important to note that the resonances at about 6.35–6.50 ppm are assigned to the anomeric proton of the glucose core.[21] The chemical shifts at 6.70–7.70 and 8.80–10.20 ppm are related to the aromatic protons and hydroxyl groups of the TA, respectively.

In $^1$H NMR spectrum of the PhATA, the aliphatic and aromatic protons of the TA core are appeared at 3.35 and 6.80 ppm, respectively. In addition, the chemical shifts at 5.90 and 7.40 ppm are corresponded to $–NH_2$ and aromatic protons of the *p*-aminobenzoate group.

In conclusion, the successful synthesis of the ThTAM macromonomer was verified by chemical shifts at 6.45 and 7.80–8.10 ppm. These chemical shifts are related to the HC=N, and aromatic protons of the thiophene rings, respectively.

### Synthesis of Star-Shaped PTh

The FTIR spectra of the PTh and star-shaped PTh are shown in Figure 4. The FTIR spectrum of the PTh shows the characteristic absorption bands due to the stretching vibrations of C=C at 1621 and 1502 $cm^{-1}$, weak aromatic $\alpha$ and $\beta$ hydrogen's of thiophene ring at 3100–2950 $cm^{-1}$ region, $\gamma$(C–H) in the aromatic ring at 1107 and 723 $cm^{-1}$, and the C–S stretching vibration at 694 $cm^{-1}$.[36,37] The FTIR spectrum of the star-shaped PTh shows similar bands with minor differences. The most distinctive feature in this spectrum is the appearance of band at 1721 $cm^{-1}$, related to the carbonyl groups of the tannic acid core.

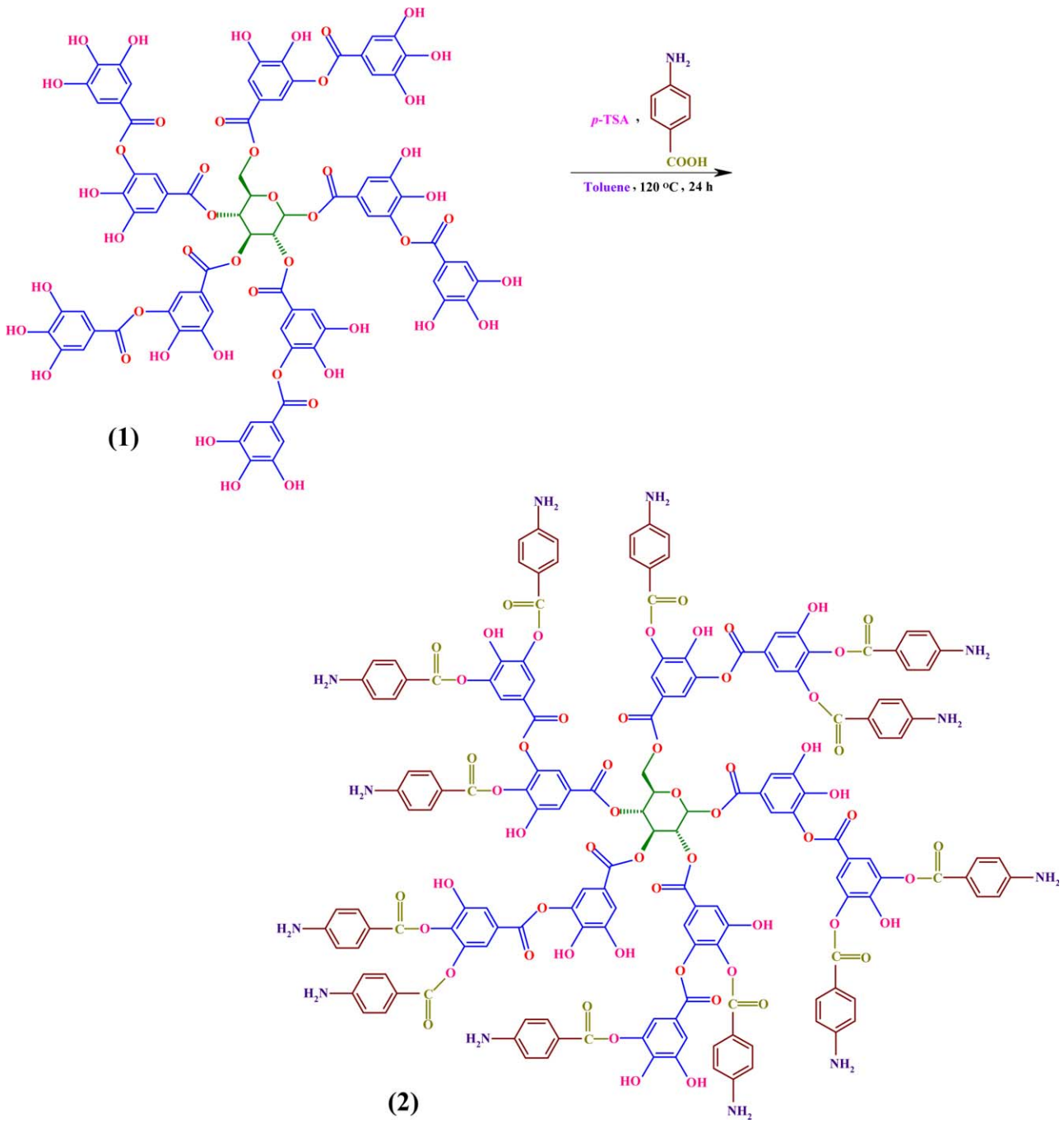


**Scheme 1.** Synthesis of phenylamine-functionalized tannic acid (PhATA). [Color figure can be viewed in the online issue, which is available at wileyonlinelibrary.com.]

### Morphology Study

The surface morphologies of the chemically synthesized PTh and star-shaped PTh were observed by means of FE-SEM. As shown in Figure 5, the PTh showed the compressed microstructure. In contrast, the synthesized star-shaped PTh exhibits the nanostructured morphology with an average diameter of $100 \pm 20$ nm. The difference morphology of the star-shaped PTh in comparison with PTh may be originated from the controlled growth of PTh chains from ThTAM macromonomer.

### Thermal Property Study

As shown in Figure 6, the thermal properties of the PTh and the synthesized star-shaped PTh were examined by means of thermogravimetric analysis (TGA) under nitrogen flow. As seen in TGA curve of the PTh, the decomposition was occurring in one step around 280 °C, and the weight loss increases rapidly from this temperature to about 750 °C. The residue at 750 °C for this sample is 35 wt %. However, the characteristic TGA thermogram of the synthesized star-shaped PTh exhibits a two-

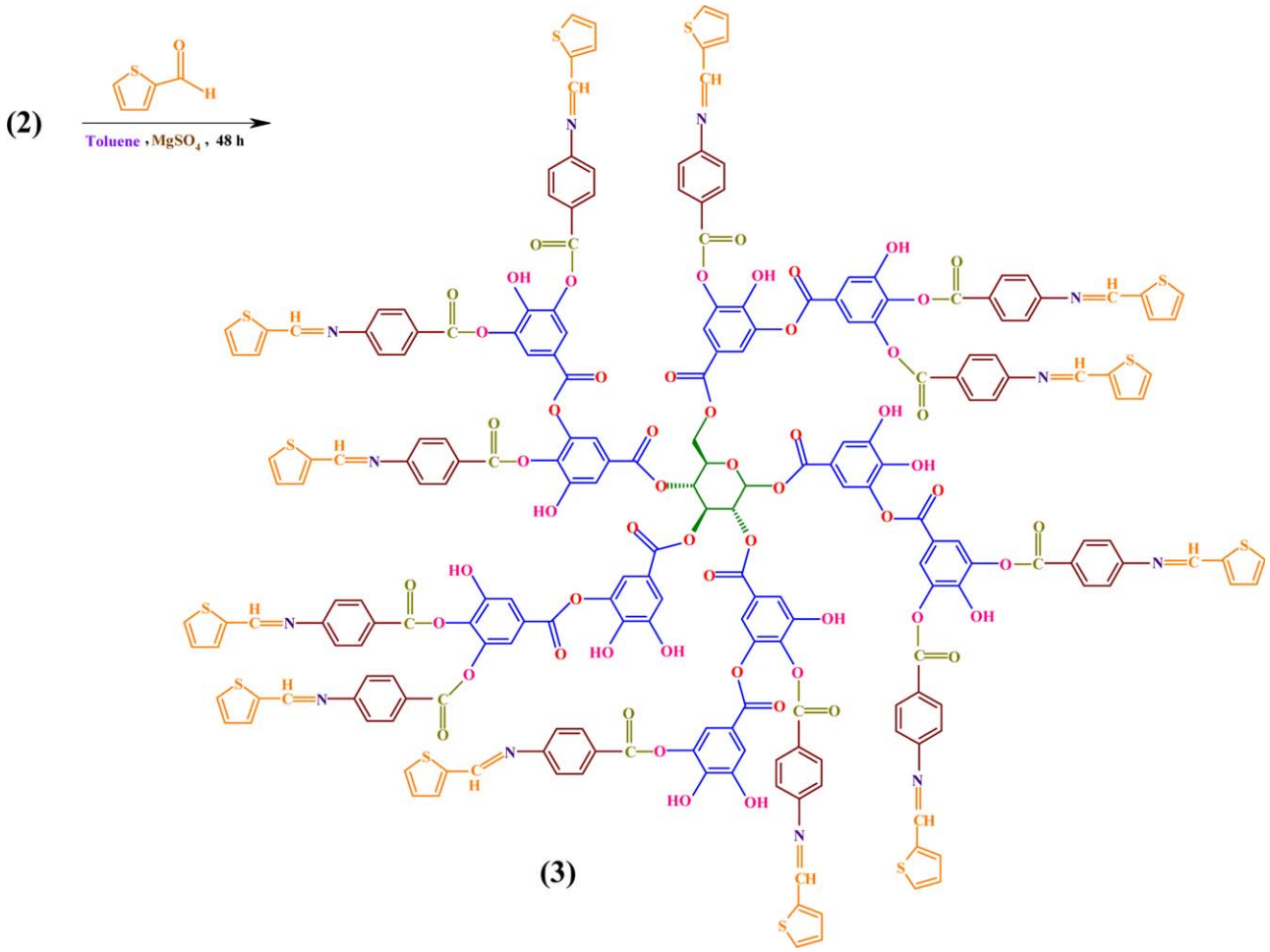


**Scheme 2.** Synthesis of thiophene-functionalized tannic acid macromonomer (ThTAM). [Color figure can be viewed in the online issue, which is available at wileyonlinelibrary.com.]

step weight loss process: the first step is related to the decomposition of the tannic acid core (220–310 °C), whereas the second step is associated with PTh chains decomposition (310–750 °C). The residue at 750 °C for the synthesized star-shaped PTh is 24 wt %. According to these results, we can draw the conclusion that the weight content of the tannic acid core in the synthesized star-shaped PTh is around 35–24 = 11 wt %.

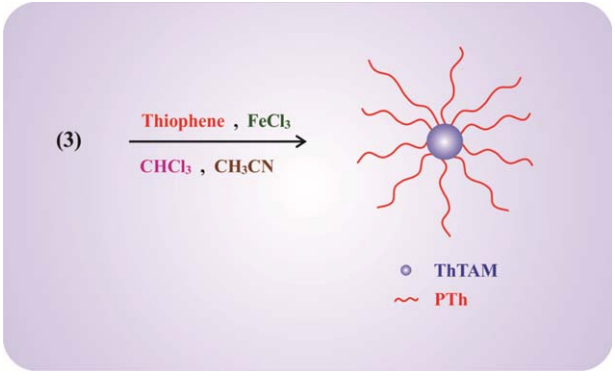


**Scheme 3.** Synthesis of star-shaped polythiophene with tannic acid core via chemical oxidation polymerization method. [Color figure can be viewed in the online issue, which is available at wileyonlinelibrary.com.]

### Solubility Test

The main drawback of un-substituted conductive polymers (e.g., PANI, PPy, and PTh) is the poor processability both in melt and solution processing. An efficient and versatile way to improving these properties in conductive polymers is structural reforms. In this respect, synthesis of star-shaped conductive polymers has been proposed as an efficient approach.[38] The solubility can be increased by reducing the compression forces in the solid state and creating new interactions between the solvent and the polymer chains by placing the substituent's on the polymer backbone.

The solubility of the synthesized PTh and star-shaped PTh in some common organic solvents were tested and the results obtained are summarized in Table I. As seen in this table, the solubility of star-shaped PTh in common organic solvents is improved in comparison with PTh. The enhanced solubility of star-shaped PTh may be originated from nanometer-sized domain growth of the polymer chains from the ThTAM macromonomer (as seen in FE-SEM image) and especially stereochemical structure of the star-shaped

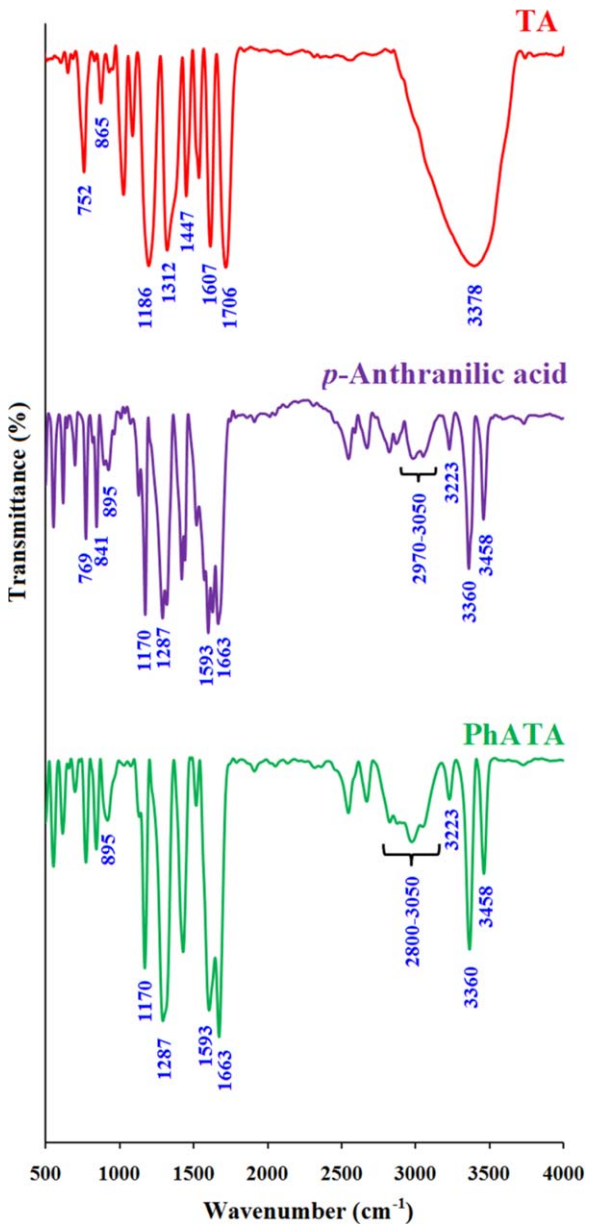


**Figure 1.** The FTIR spectra of the tannic acid, *p*-anthranilic acid, and PhATA. [Color figure can be viewed in the online issue, which is available at wileyonlinelibrary.com.]

PTh. However, lower compression forces in the solid state of the star-shaped PTh may be another reason for the enhanced solubility. It should be pointed out that, the tannic acid core in the case of star-shaped PTh is the another factor in the enhanced solubility in comparison with PTh.

In addition, as seen in Table I, the electrochemically synthesized star-shaped PTh, under condition as given in the Experimental section, showed lower solubility than those of the corresponding chemically synthesized sample.

### Electroactivity Measurements

Similar to most of the conducting polymers (e.g., polyaniline, polypyrrole, and polyfuran), the PTh can be synthesized by both chemical and electrochemical oxidation polymerization methods.[39–42] In addition, it is well established that, the electrochemical process is more advantageous since film properties such as conductivity and thickness can be controlled by the electrochemical parameters such as current density, substrate, pH, nature, and concentration of electrolyte. Furthermore, in electrochemical method, the polymer is enabling to simultaneous doping and entrapment of small molecules.[1]

After electropolymerization under identified conditions, as given in the Experimental section, the electroactivity behaviors of the synthesized samples (PTh and star-shaped PTh) were studied under cyclic voltammetric conditions. The effect of the potential scanning rate (V) on the peak currents for the PTh and star-shaped PTh in the range of 25 to 150 mV $s^{-1}$ scan rate, in the acetonitrile–tetraethylammonium tetrafluoroborate (TEAFB), solvent–electrolyte couple (0.1 mol $l^{-1}$) between −0.20 and +1.70 V under argon atmosphere are shown in Figure 7. All potentials are given versus the reference Ag/AgCl electrode. As shown in Figure 7(a), the cyclic voltammograms (CVs) of the PTh shows a typical redox couple with anodic and cathodic peaks at approximately 1.00 and 0.75 V versus Ag/AgCl electrode, respectively. In addition, the anodic

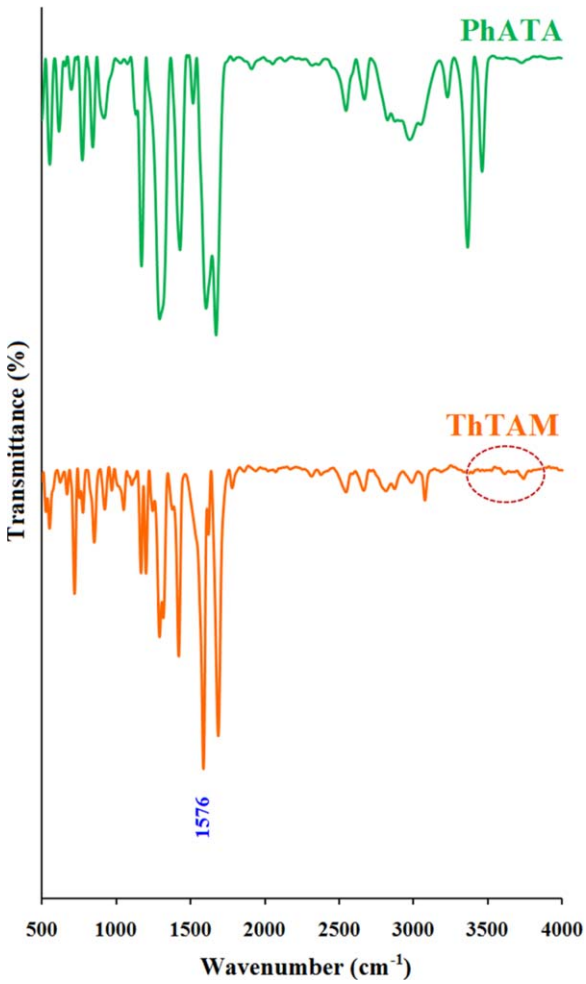


**Figure 2.** The FTIR spectra of the PhATA and ThTAM. [Color figure can be viewed in the online issue, which is available at wileyonlinelibrary.com.]

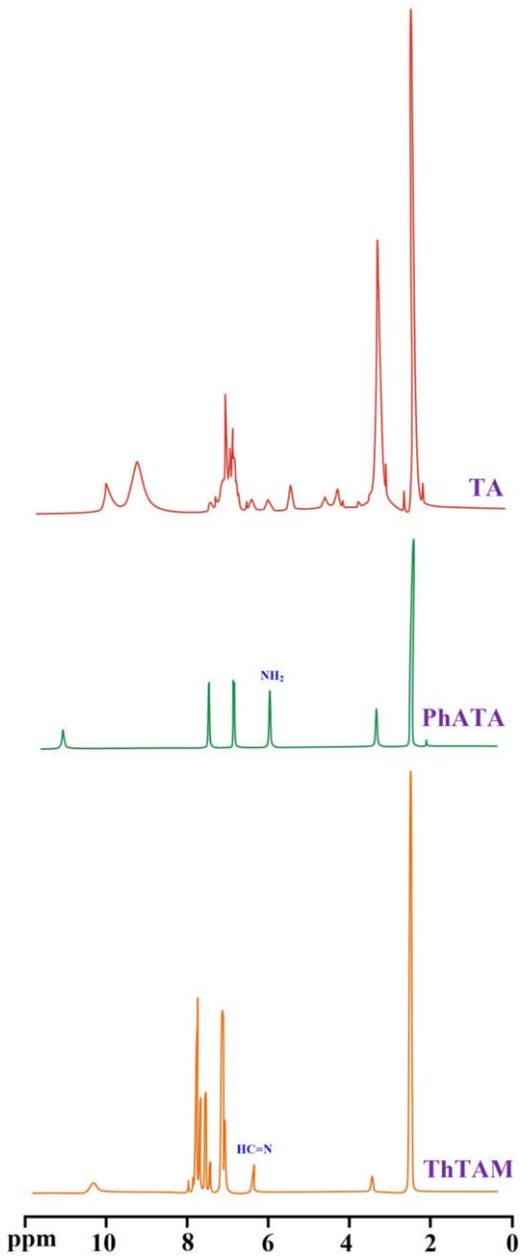


Figure 3. The $^{1}$H NMR spectra of the TA, PhATA, and ThTAM. [Color figure can be viewed in the online issue, which is available at wileyonlinelibrary.com.]

peaks shifts in the direction of positive potential (0.90 to 1.10) with increasing scan rate, which indicates the electrochemical oxidation/reduction (doping/dedoping) of the deposited PTh film onto Pt electrode was chemically reversible.

As seen in Figure 7(b), the cyclic voltammograms (CVs) of the star-shaped PTh exhibits some qualitative similarities to those of the PTh. The CVs of the star-shaped PTh shows a typical redox couple with anodic and cathodic peaks at approximately 1.15 and 0.73 V versus Ag/AgCl electrode, respectively. Moreover, similar to PTh, the anodic peaks shifts in the direction of positive potential (1.00 to 1.30 V) with increasing scan rate, which indicates the electrochemical oxidation/reduction (doping/dedoping) of the deposited star-shaped PTh film onto Pt electrode was chemically reversible.

For additional evidence on the redox stability, the cyclic voltammograms (5 cycles) of the star-shaped PTh are recorded between −0.20 and +1.70 V versus Ag/AgCl electrode at a scan rate of 200 mV $s^{-1}$. As shown in Figure 7(c), the oxidation and reduction peak currents are observed at approximately 1.20 and 0.77 V versus Ag/AgCl, respectively. These CVs revealed that the synthesized star-shaped PTh still retained good redox activity and the resulting polymer is highly stable.

To evaluate the electroactivity further, the relationship between the peak current sizes (anodic peaks) versus scan rate was determined. The linear relationships between the current and scan rate in the range of 25 to 150 mV $s^{-1}$ for the PTh and star-shaped PTh are shown in Figure 7(d). This linear relationship is typical of redox-active polymers attached to the electrodes and also exemplifies the stability of the synthesized samples toward doping/dedoping.

**Electrical Conductivity Measurement**

The $\pi$-conjugated polymers in general and polythiophene(s) in particular are considered as potential candidates for electrical applications, in part due to their electrical conductivities and environmental stabilities. However, it is well established that the electrical conductivity of PTh depends on the synthesis parameters such as type of solvent, type and ratio of oxidant, temperature, and reaction time.[43] The electrical conductivities of the

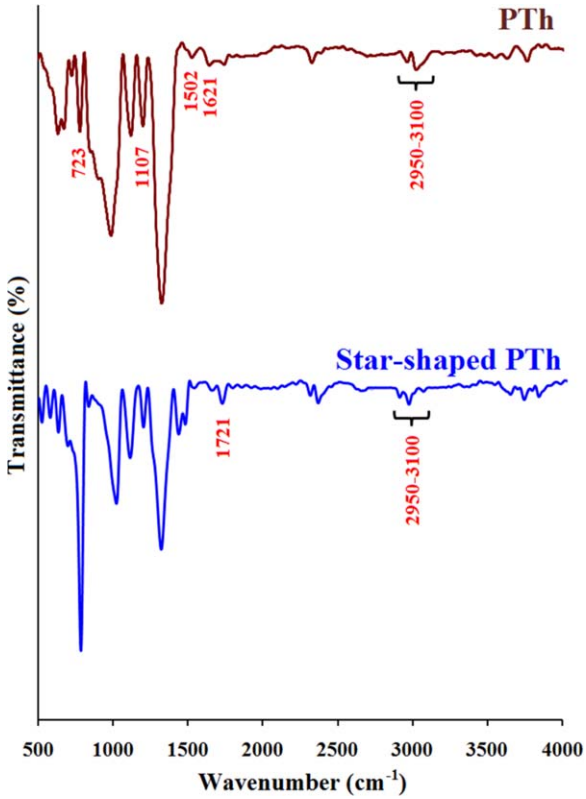


Figure 4. The FTIR spectra of the PTh and star-shaped PTh. [Color figure can be viewed in the online issue, which is available at wileyonlinelibrary.com.]

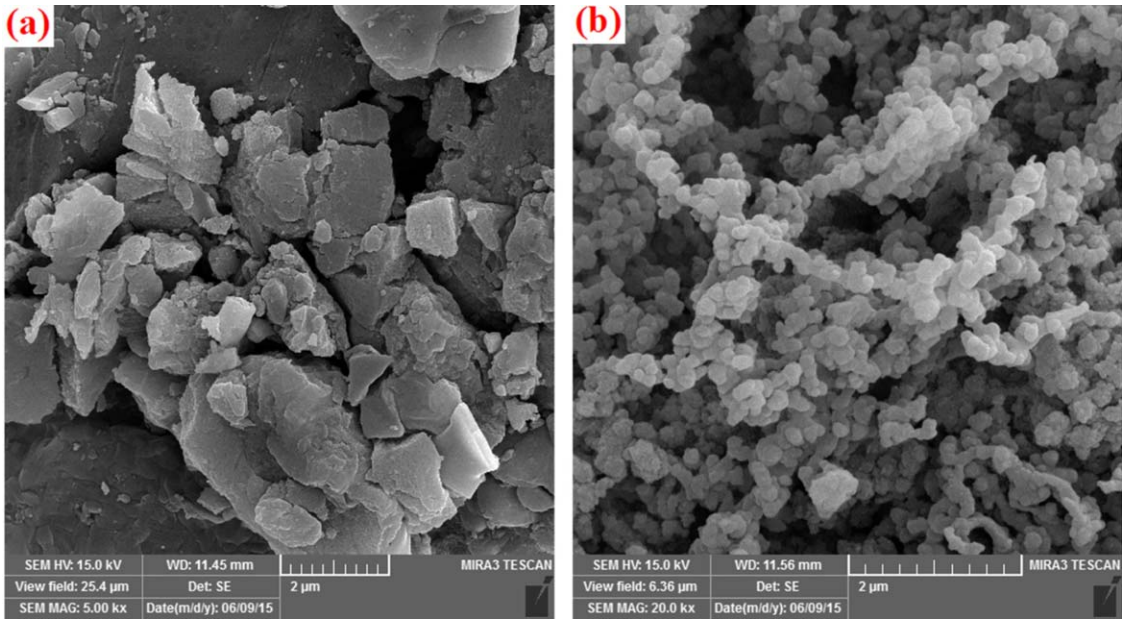


**Figure 5.** The FE-SEM images of the synthesized (a) PTh and (b) star-shaped PTh. [Color figure can be viewed in the online issue, which is available at wileyonlinelibrary.com.]

synthesized samples were measured by the four-probe technique at room temperature. It should be pointed out that the experimental determinations were repeated 5 times for each sample to evaluate the sample accuracy.

Using the values of voltage ($V$), current ($I$), and thicknesses (d) of the samples, the volume specific resistivities ($\rho$; Ω cm), and subsequently, the electrical conductivities ($\sigma$; S $cm^{-1}$) of the samples were calculated using the following equations.

$$\rho = (V/I)\ (\pi/\ln 2)\mathrm{d}$$

$$\sigma = 1/\rho$$

The electrical conductivity results obtained are listed in Table II. As shown in this table, the electrochemically synthesized samples show higher electrical conductivities than those of the chemically synthesized samples.

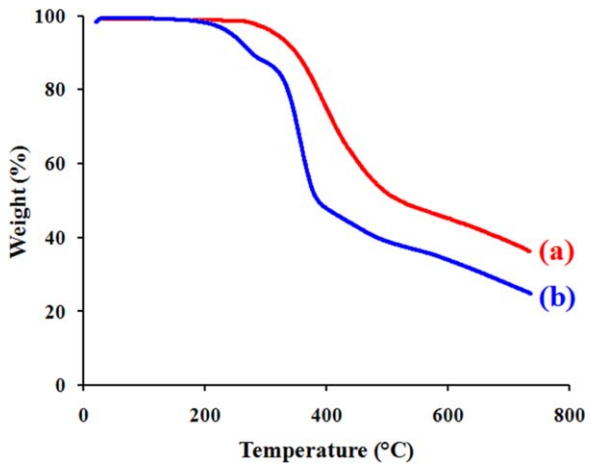


**Figure 6.** TGA thermograms of the (a) PTh and (b) star-shaped PTh. [Color figure can be viewed in the online issue, which is available at wileyonlinelibrary.com.]

According to the results obtained from electrical conductivity and electroactivity studies, the conclusion could be drawn that the synthesized star-shaped PTh has higher electrical conductivity and electroactivity than those of the PTh. These results originated from the spherical, three-dimensional, and nanostructure morphology of the star-shaped PTh, which allows sufficient overlapping of π-orbitals.

### UV–Vis Spectroscopy

The optical properties of the PTh and star-shaped PTh samples were investigated by means of ultraviolet–visible (UV–vis) spectroscopy. The samples for UV–vis spectroscopy were prepared by dissolving the same amount of the samples in *N*-methylpyrrolidone (NMP) followed by ultrasonic treatment for 15 min. Figure 8 depicts the UV–vis spectra of the PTh and star-shaped PTh samples. As seen in this figure, the UV–visible spectrum of the PTh was characterized by a broad electronic transition centered at about 530 nm. In contrast, the UV–vis spectrum of the star-shaped PTh was characterized by two electronic transitions at about 317 and 585 nm.

## CONCLUSIONS

The nanostructured star-shaped polythiophene with tannic acid core via a "core-first", and both chemical and electrochemical oxidation polymerization methods were successfully synthesized and characterized, which was never reported in the past. The synthesized star-shaped PTh showed higher electrical conductivity and electroactivity than those of the PTh in both chemical and electrochemical polymerized samples, due to its large surface area, spherical, and three-dimensional structure, and sufficient intermolecular and π-orbitals overlaps. The synthesized

**Table I.** Solubility of PTh and Star-Shaped PTh in Some Common Organic Solvents

| Solvent | DMSO | DMF | NMP | THF | $CHCl_3$ | Xylene |
|---|---|---|---|---|---|---|
| Chemically synthesized PTh | + | + | + | – | – | – |
| Chemically synthesized star-shaped PTh | ++ | ++ | ++ | + | – | – |
| Electrochemically synthesized PTh | + | + | + | – | – | – |
| Electrochemically synthesized star-shaped PTh | + | + | + | – | – | – |

++, sparingly soluble; +, slightly soluble; –, insoluble; the concentration used in the solubility test was 10 mg of each polymer in 1 mL of solvents at room temperature; DMSO, dimethylsulfoxide; DMF, *N*,*N*-dimethylformamide; NMP, *N*-methylpyrrolidone; THF, tetrahydrofuran.

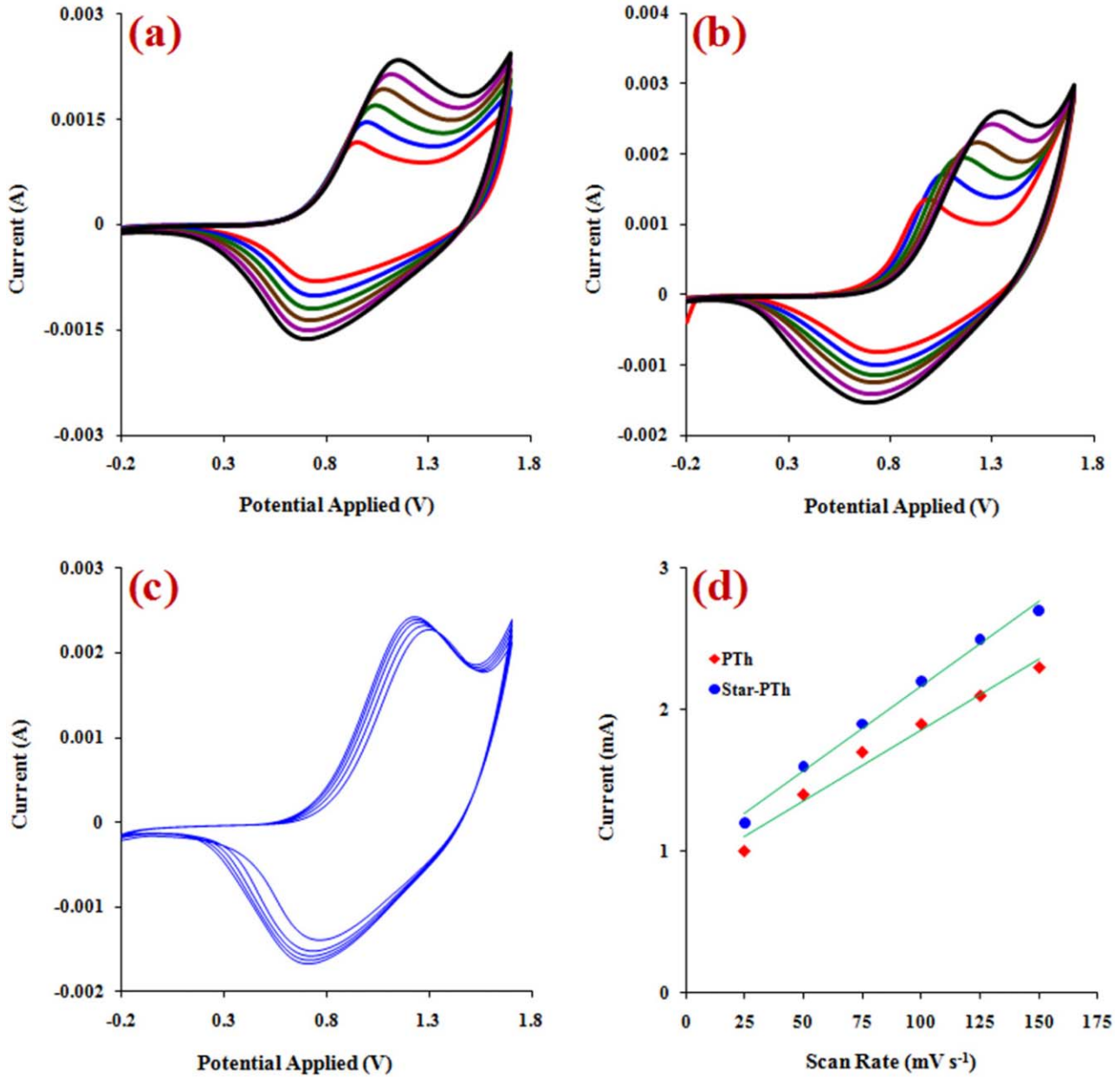


**Figure 7.** Cyclic voltammetry (CVs) curves of the (a) electrochemically deposited PTh, (b) electrochemically deposited star-shaped PTh, and (c) cyclic voltammograms (5 cycles) of the star-shaped PTh at a scan rate of 200 mV $s^{-1}$ in a acetonitrile–tetraethylammonium tetrafluoroborate (TEAFB), solvent–electrolyte couple (0.1 mol $L^{-1}$), and (d) the effect of the potential scanning rate (V) on the peak currents for the PTh, and star-shaped PTh in the range of 25 to 150 mV $s^{-1}$ scan rate. [Color figure can be viewed in the online issue, which is available at wileyonlinelibrary.com.]

**Table II.** The Electrical Properties of the Synthesized Samples

| Sample | Volume specific resistivity ($\rho$; Ω cm) | Electrical conductivity ($\sigma$; S $cm^{-1}$) |
|---|---|---|
| Electrochemically synthesized PTh | 0.53 | 1.90 |
| Chemically synthesized PTh | 0.85 | 1.17 |
| Electrochemically synthesized star-shaped PTh | 0.43 | 2.32 |
| Chemically synthesized star-shaped PTh | 0.67 | 1.49 |

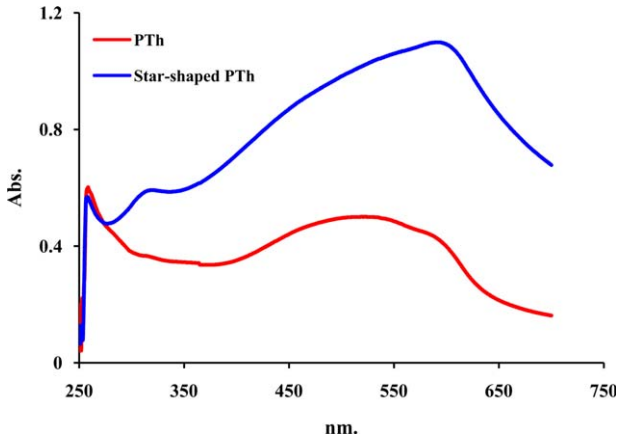


**Figure 8.** The UV–vis spectra of the PTh and star-shaped PTh in *N*-methylpyrrolidone (NMP) solution. [Color figure can be viewed in the online issue, which is available at wileyonlinelibrary.com.]

star-shaped PTh can be used in organic electronics such as light-emitting diodes (OLEDs), field-effect transistors (OFETs), electrochromic devices, sensors, photovoltaic cells, lasers, and batteries, in part owing to its durability, resilience, good redox activity, and proven electrical conductivity.

Moreover, due to natural origin and biocompatibility of the tannic acid core, the blend of star-shaped PTh with biodegradable and biocompatible polymers can be considered as a prospective candidate for biomedical applications such as tissue engineering. In conclusion, further experiments are under progress in order to evaluate the influence of the synthesis conditions such as current density, substrate, pH, nature and concentration of electrolyte in electrochemical oxidation polymerization method, and type of oxidant, reaction time, and temperature in chemical oxidation polymerization method on the physicochemical properties of the synthesized samples.

## ACKNOWLEDGMENTS

We express our gratitude to the Payame Noor University and Research Center for Pharmaceutical Nanotechnology, Tabriz University of Medical Sciences for supporting this project.

## REFERENCES

1. Jaymand, M.; Hatamzadeh, M.; Omidi, Y. *Prog. Polym. Sci.* **2015**, *47*, 26.
2. Jaymand, M. *Prog. Polym. Sci.* **2013**, *38*, 1287.
3. Massoumi, B.; Hosseinzadeh, M.; Jaymand, M. *J. Mater. Sci. Mater. Electron.* **2015**, *26*, 6057.
4. Howard, I. A.; Mauer, R.; Meister, M.; Laquai, F. *J. Am. Chem. Soc.* **2010**, *132*, 14866.
5. Routh, P. K.; Nykypanchuk, D.; Venkatesh, T. A.; Cotlet, M. *Adv. Funct. Mater.* **2015**, *25*, 5902.
6. Liu, P.; Wu, Y.; Pan, H.; Ong, B. S.; Zhu, S. *Macromolecules* **2010**, *43*, 6368.
7. Hu, D.; Zhang, L.; Zhang, K.; Duan, X.; Xu, J.; Dong, L.; Sun, H.; Zhu, X.; Zhen, S. *J. Appl. Polym. Sci.* **2015**, *132*, 41559.
8. Tian, C.; Du, Y.; Xu, P.; Qiang, R.; Wang, Y.; Ding, D.; Xue, J.; Ma, J.; Zhao, H.; Han, X. *ACS Appl. Mater. Interf.* **2015**, *7*, 20090.
9. Wang, A.; Zhou, X.; Qian, T.; Yu, C.; Wu, S.; Shen, J. *Appl. Phys. A* **2015**, *120*, 693.
10. Li, Y.; Nese, A.; Hu, X.; Lebedeva, N. V.; LaJoie, T. W.; Burdynska, J.; Stefan, M. C.; You, W.; Yang, W.; Matyjaszewski, K.; Sheiko, S. S. *ACS Macro Lett.* **2014**, *3*, 738.
11. Samsonidze, G.; Ribeiro, F. J.; Cohen, M. L.; Louie, S. G. *Phys. Rev. B* **2014**, *90*, 035123.
12. Jo, J. W.; Jung, J. W.; Wang, H. W.; Kim, P.; Russell, T. P.; Jo, W. H. *Chem. Mater.* **2014**, *26*, 4214.
13. Zhang, H.; Hu, Z.; Li, M.; Hu, L.; Jiao, S. *J. Mater. Chem. A* **2014**, *2*, 17024.
14. Huynh, T. P.; Sharma, P. S.; Sosnowska, M.; D'Souza, F.; Kutner, W. *Prog. Polym. Sci.* **2015**, *47*, 1.
15. Lanzi, M.; Salatelli, E.; Benelli, T.; Caretti, D.; Giorgini, L.; Di-Nicola, F. P. *J. Appl. Polym. Sci.* **2015**, *132*, 42121.
16. Shao, M.; He, Y.; Hong, K.; Rouleau, C. M.; Xiao, D. B. G. K. *Polym. Chem.* **2013**, *4*, 5270.
17. Aydin, M.; Esat, B. *J. Solid. State. Electrochem.* **2015**, *19*, 2275.
18. Burroughes, J. H.; Bradley, D. D. C.; Brown, A. R.; Marks, R. N.; Mackay, K.; Friend, R. H.; Burns, P. L.; Holmes, A. B. *Nature* **1990**, *347*, 539.
19. Li, Y. S.; Zhang, Y.; Wu, X.; Wang, X.; Wang, F. Z. *Macromol. Chem. Phys.* **2015**, *216*, 113.
20. Das, S.; Chatterjee, D. P.; Ghosh, R.; Nandi, A. K. *RSC Adv.* **2015**, *5*, 20160.
21. Massoumi, B.; Sorkhi-Shams, N.; Jaymand, M.; Mohammadi, R. *RSC Adv.* **2015**, *5*, 21197.
22. Metin, A.; Toppare, L. *Mater. Chem. Phys.* **2009**, *114*, 789.
23. Casado, J.; Pappenfus, T. M.; Mann, K. R.; Hernandez, V.; Navarrete, J. T. L. *J. Chem. Phys.* **2004**, *120*, 11874.
24. Ponnapati, R.; Felipe, M. J.; Park, J. Y.; Vargas, J.; Advincula, R. *Macromolecules* **2010**, *43*, 10414.
25. Behbahani, M.; Bide, Y.; Salarian, M.; Niknezhad, M.; Bagheri, S.; Bagheri, A.; Nabid, M. R. *Food Chem.* **2014**, *158*, 14.

26. Baleg, A. A. A.; Jahed, N. M.; Arotiba, O. A.; Mailu, S. N.; Hendricks, N. R.; Baker, P. G.; Iwuoha, E. I. *J. Electroanal. Chem.* **2011**, *652*, 18.
27. Jarosz, T.; Lapkowski, M.; Ledwon, P. *Macromol. Rapid Commun.* **2014**, *35*, 1006.
28. Monnin, A. F.; Buron, C. C.; Guyard, L.; Charraut, D.; Salut, R.; Filiâtre, C. *Synth. Met.* **2012**, *162*, 1.
29. Xia, C.; Fan, X.; Locklin, J.; Advincula, R. C. *Org. Lett.* **2002**, *4*, 2067.
30. Deng, S.; Krueger, G.; Taranekar, P.; Sriwichai, S.; Zong, R.; Thummel, R. P.; Advincula, R. C. *Chem. Mater.* **2011**, *23*, 3302.
31. Deng, S.; Advincula, R. C. *Macromol. Rapid Commun.* **2011**, *32*, 1634.
32. Wu, D. T. *Synth. Met.* **2002**, *126*, 289.
33. Liu, Y.; Guo, X.; Xiang, N.; Zhao, B.; Huang, H.; Li, H.; Shen, P.; Tan, S. *J. Mater. Chem.* **2010**, *20*, 1140.
34. Apodaca, D. C.; Pernites, R. B.; Ponnapati, R. R.; Mundo, F. R. D.; Advincula, R. C. *ACS Appl. Mater. Interf.* **2011**, *3*, 191.
35. Sayed, G. H.; Ghuiba, F.; Abdou, M.; Badr, M. I.; Tawfik, E. A. A.; Negm, S. M. N. A. M. *Colloid. Surf. A* **2012**, *393*, 96.
36. Hatamzadeh, M.; Jaymand, M. *RSC Adv.* **2014**, *4*, 16792.
37. Massoumi, B.; Jaymand, M. *J. Mater. Sci. Mater. Electron.* **2016**, *27*, 2267.
38. Chu, C. C.; Wang, Y. W.; Wang, L.; Ho, T. I. *Synth. Met.* **2005**, *153*, 321.
39. Hatamzadeh, M.; Mahyar, A.; Jaymand, M. *J. Braz. Chem. Soc.* **2012**, *23*, 1008.
40. Jaymand, M. *Design. Monomer. Polym.* **2011**, *14*, 433.
41. Wang, J.; Krishna, R.; Wu, X.; Sun, Y.; Deng, S. *Langmuir* **2015**, *31*, 9845.
42. Jaymand, M. *RSC Adv.* **2014**, *4*, 33935.
43. Wen, L.; Jeong, D. C.; Javid, A.; Kim, S.; Nam, J. D.; Song, C.; Han, J. G. *Thin Solid Film.* **2015**, *587*, 66.